HIGHLY DAMPED GR/MG COMPOSITES FOR FLEXIBLE SPACE STRUCTURES

Uday Kashalikar
Joseph Boyce
Foster-Miller, Inc., Waltham, MA
(617) 890-3200

ABSTRACT

Structures for space-based weapons must possess a high vibrational damping for effective defense against a multiple missile threat. Development of an ultrastiff material ($E/\rho > 8 \times 10^8$ in.) with high inherent damping capacity ($\psi > 2$ percent) in the high frequency-low strain region will improve performance and reliability of the system, and reduce the need for active damping.

The Interfacial Slip Damping (ISD) mechanism consists of dissipating frictional energy at the fiber/matrix interface under external dynamic loading. In case of Gr/Mg composites, the fabrication residual stresses and the interface frictional coefficient must be reduced in order to promote energy dissipation by controlled interfacial slip rather than initiation and/or propagation of matrix cracks. The ISD phenomenon is effective even at low strain levels ($<10^{-5}$) which is essential for a fast decay of free structural vibrations to an acceptable amplitude. A 150 percent improvement in damping was achieved with P-55 Gr/Mg composite (from $\psi = 1.6$ percent to $\psi = 4$ percent), by promoting the ISD mechanism.

Advanced space structures will benefit from this technology in the following ways:

- Damping - Large improvements in strain-independent damping. A simplified model predicts that close to an order of magnitude improvement in damping is achievable with <5 percent reduction in stiffness of Gr/Mg metal matrix composite (MMC).
- Specific stiffness - High fiber content ($v_f > 60$ percent) will result in an outstanding specific stiffness ($>9 \times 10^8$ in. with 100-Msi reinforcement).
- Cost - Reduced requirement for active damping will lower structural cost.

This research was sponsored by SDIO/IST and managed by NSWC.

INTRODUCTION

Continuous fiber-reinforced MMCs are well-suited for space structural applications because they typically possess a high specific stiffness, a near-zero coefficient of thermal expansion (CTE) and a good resistance to the space environment. In addition, flexible space structures such as the Space Based Laser (SBL) will require structural materials with a high inherent damping to achieve the requisite dynamic dimensional precision. The SBL is intended to destroy a large number of target missiles in a very brief period of time, which will require rapid retargeting and accurate firing capability. The short "readiness-to-fire" time for the SBL dictates that the vibrations induced under the inertial retarget loads must be damped quickly. As presented in Figure 1, the settling period of free vibrations will largely control the effectiveness of the SBL weapon. During this research, a significant improvement in the settling time was demonstrated in Gr/Mg MMCs through an innovative processing technique.

For a specified value of the acceptable amplitude, α_s, the settling period can be shortened by increasing:

- Material and structural damping
- Specific stiffness
- Natural frequency of the structure.

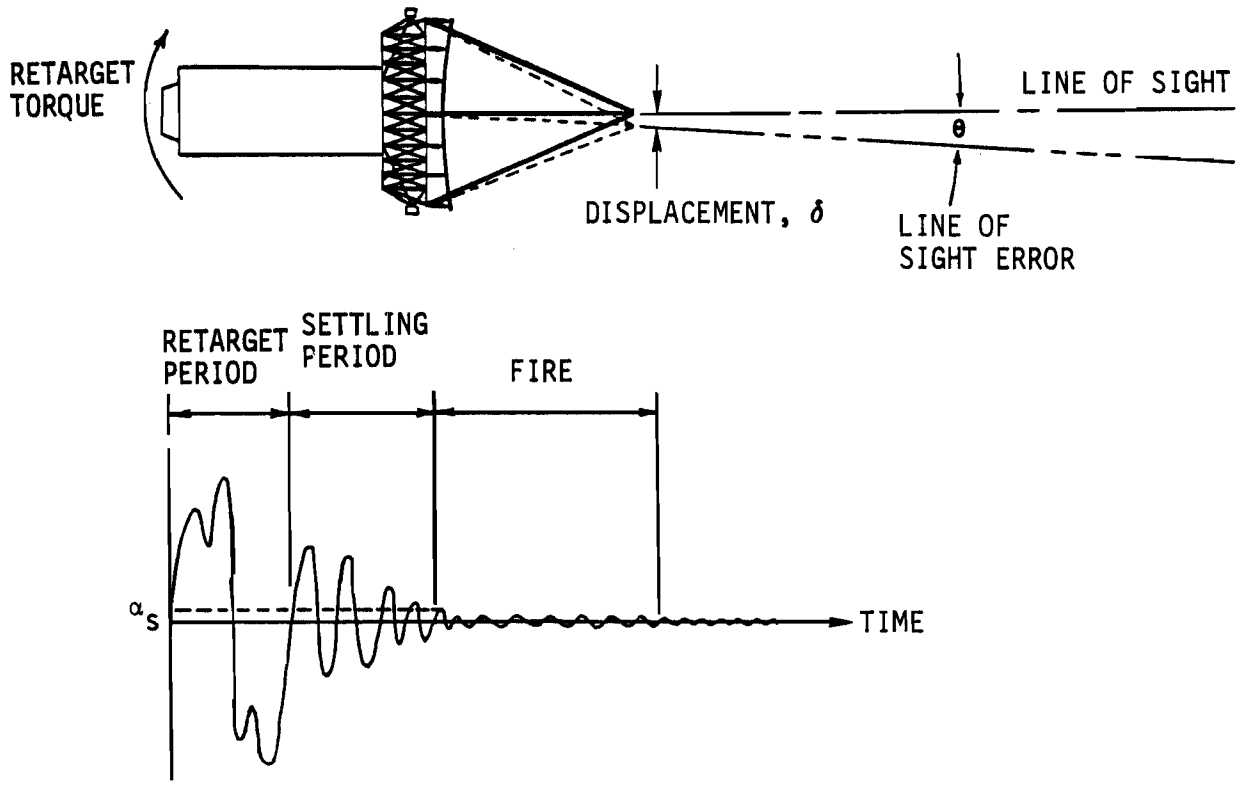

Figure 1. SBL Performance Simulation[1]

The damping behavior of continuous fiber MMCs has been reviewed by Timmerman,[2] Mishra,[3] and Steckel.[4] Various measures of damping have been reported such as loss factor (η), loss angle (ϕ), logarithmic decrement (δ), quality factor (Q), specific damping capacity (ψ) and damping ratio (ζ). In this paper, specific damping capacity, ψ, will be used as a measure of material damping. At low damping levels (i.e., $\eta < 1$), these damping parameters are interrelated by the following expression:

$$Q^{-1} = \eta = \tan\Theta = \Theta = E_I/E_R$$

$$= \delta/\pi = \psi/2\pi = \Delta W/2\pi W = 2\zeta$$

Damping properties of materials are a function of temperature, frequency, static preload and material strain. The effect of these parameters on damping in viscoelastic materials is described in Reference 5. Generally, at low stress or strain ($<10^{-6}$) levels, the damping behavior of a material is independent of stress amplitude, but depends on frequency and temperature. At intermediate stress or strain (10^{-6} to 10^{-3}) levels of engineering interest, polymeric materials still exhibit linear damping, but the damping capacity of metals and alloys increases with increasing stress amplitude and is independent of frequency and temperature. Various energy dissipation mechanisms at these stress levels involve movement of dislocations or interfaces such as magnetic domain walls, twin boundaries, or martensite invariants.

In the case of MMCs, the interface is a region of imperfections (voids, disbonds) and residual stresses. Most of the energy dissipation occurs in this region, and can be attributed to interaction between the constituents rather than the constituents themselves. This postulation is supported by the fact that damping in most MMCs is greater than the inherent damping in fiber and matrix phases.[3]

The effect of strain on damping in graphite fiber MMCs has been investigated by Martin Marietta[6], and the qualitative results are presented in Figure 2. The total damping capacity (ψ_{total}) of MMCs may be expressed as a sum of its strain-independent (ψ_I) and strain-dependent (ψ_H) components. While the linear strain-independent component exists at all strain levels, the nonlinear strain-dependent component is reduced to zero at low strain levels ($<10^{-5}$).

Strain-Independent Damping:

At low strain amplitude ($<10^{-5}$) where damping is independent of strain but depends on frequency, the energy dissipation is primarily a result of mechanisms involving atomic diffusion or Zener's thermoelastic effect.[7,8] In the case of composites, frictional energy can be dissipated due to relative motion between fiber and matrix phases. This is especially applicable to MMCs, where fiber/matrix bonding is mechanical rather than chemical. Interfacial slip can be promoted in MMCs by proper control of fabrication residual stresses and interface coefficient of friction, as demonstrated during this program. Strain-independence and frequency-dependence features of the ISD mechanism were verified during this research.

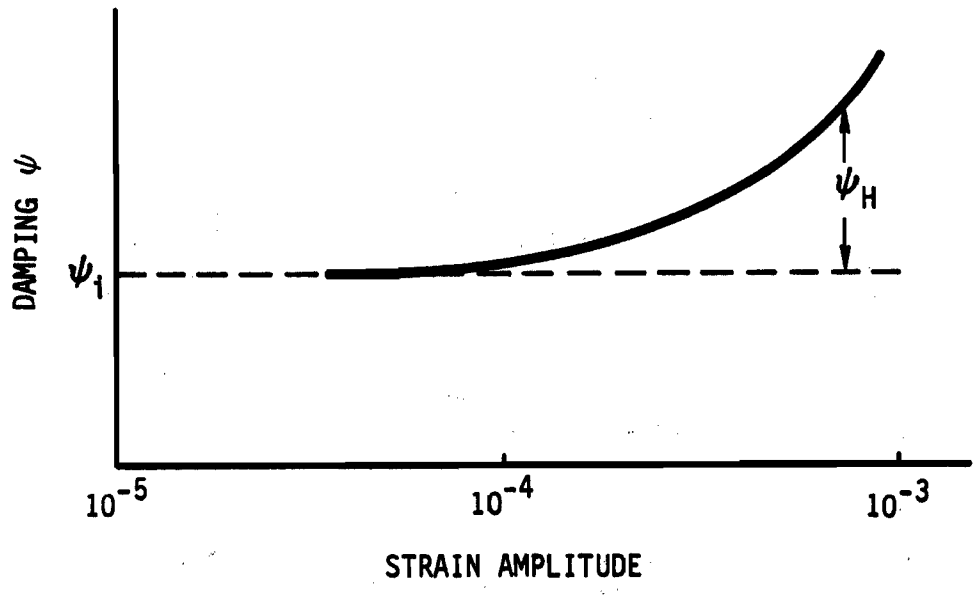

Figure 2. Strain-Dependence Behavior of MMC Damping[6]

Strain-Dependent Damping:

At intermediate strain levels (10^{-5} to 10^{-3}), the nonlinear strain-dependent damping (ψ_H) may involve hysteretic losses resulting from local yielding of the matrix under cyclic stress. At the microstructural level, the energy dissipation may involve a breakaway dislocation mechanism as envisioned by the Granato-Lucke (G-L) model.[2] Martin Marietta has researched the dislocation damping mechanism in Gr/Al[6], as well as Gr/Mg[9] composites, and has achieved significant improvement in strain-dependent damping by promoting this mechanism.

Table 1 presents the major characteristics of ISD and dislocation damping mechanisms. While dislocation damping offers higher payoffs at intermediate strains, interfacial slip enhances damping in the low strain region as well. Thus, effective application of both mechanisms is critical in improving dynamic dimensional precision of flexible space structures.

The objective of this research was to significantly shorten the settling period of free vibrations for Gr/Mg MMCs. This overall objective was to be achieved through:

- Enhanced material damping by promoting a controlled interfacial slip under external loading
- Increased specific stiffness.

Table 1. Primary Damping Mechanisms in MMCs

Characteristic	Interfacial Slip	Dislocation Damping
1. Effectiveness at low strain level ($<10^{-5}$)	Yes, ψ = 4 percent demonstrated	Not effective
2. Effectiveness at 10^{-5} to 10^{-3} strain	Yes, as above	More effective than interfacial slip[9]
3. Frequency, temperature dependency	Likely, must be investigated	None
4. Miscellaneous advantages (projections)	• Lower residual stresses will inhibit propagation of matrix cracks, hence improve fatigue strength, transverse strength • No limitations on choice of matrix alloy • Fiber coating can reduce stress concentration, hence increase transverse strength	• No interface wear
5. Miscellaneous concerns (projections)	• Wear at fiber/matrix • Effect of coating on longitudinal stiffness	• Limited to alloys with low σ_y (more dislocation prone) • High residual stresses (due to CTE mismatch) essential to form dislocations - Can promote matrix cracks, hence lower fatigue strength transverse strength

Conventional processing techniques produce Gr/Mg composites with high fabrication related interface residual stresses as a result of the mismatch in CTE of the two phases. The CTE of the magnesium alloy matrix is larger than the CTE of graphite fibers in the radial direction. Thus, as the composite cools down to room temperature, the matrix clamps down on the embedded graphite fibers. Compressive residual stresses in excess of 15 Ksi are predicted at the fiber/matrix interface.[10] Considering the coefficient of sliding fraction, μ to be 0.5 (typical for graphite on metal), interface tangential stresses close to 10^4 psi are required to overcome the frictional force and cause the fiber to slip. Until this stress level is attained, there is no fiber slippage, and the input energy must be stored as strain energy in the matrix. When the matrix cannot sustain any further strain energy, matrix cracks will be initiated. Thus, the stress level to permit interfacial slip will never develop in the MMC. Instead, the matrix cracks will propagate, leading to failure. Thus, the high interface frictional force is believed to result in low damping, low fatigue strength, low damage tolerance, and low toughness in MMCs. During this research, interface slip was promoted by lowering the residual stresses using a specialized processing technique.

RESEARCH AND RESULTS

Several P-55 Gr/Mg 10 Al specimens were fabricated using a proprietary pressure casting approach. Some of the MMC specimens are shown in Figure 3. The flat specimens consisted of control specimens and specially processed zirconia-dispersed specimens. The fine zirconia particulate dispersion was expected to reduce the residual stresses in the composite as a result of its low effective modulus. The MMC specimens were evaluated through microscopy, tensile tests and vibrational tests.

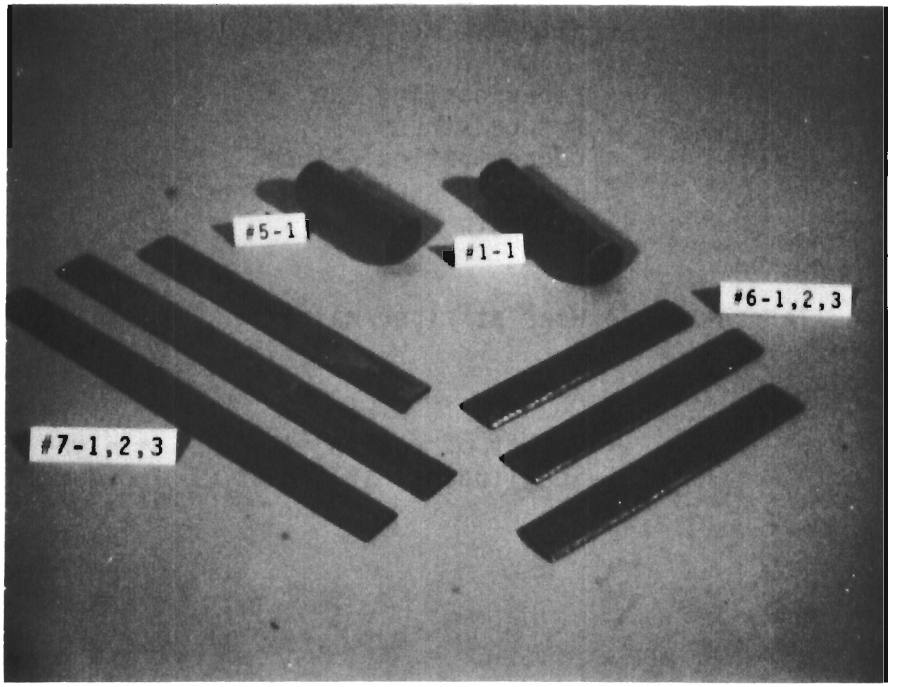

Figure 3. Tubular and Flat MMC Specimens

Microscopy Results:

Figure 4 is an optical micrograph showing a representative cross section of the control specimen. By areal measurement fiber content was estimated at 63 volume percent. The fiber distribution is uniform - "channeling" was avoided in all specimens through a high fiber content. Also evident is the excellent infiltration, as indicated by absence of voids in this specimen. Figure 5 presents scanning electron micrographs (SEMs) of the same specimen at a higher magnification (600 times). Again, the high fiber content can be noted. The micrograph in Figure 5 shows a few small (<1μ) voids present at fiber periphery. These voids appear to be shrinkage cavities (rather than uninfiltrated regions). The shrinkage cavities are a result of using a preheated fiber preform, which causes matrix solidification to occur last at the fiber surfaces. This problem can be reduced through improved directional solidification schemes and by reducing the preform temperature during infiltration.

Figure 6 is an SEM of a zirconia-dispersed Gr/Mg specimen. The ultrafine zirconia particles (0.15μ size) have coalesced into white zirconia regions around the graphite fibers. Zirconia particles have lodged between the graphite fibers, reducing the number of fiber-to-fiber contact points. This is expected to improve MMC transverse strength. Also, slip regions are evidenced at fiber matrix interface, promoted by reduced residual stresses in that region. In this case, the slip has occurred to relieve the compressive residual stresses along the fiber (due to negative fiber CTE). This is called the Bauschinger effect.

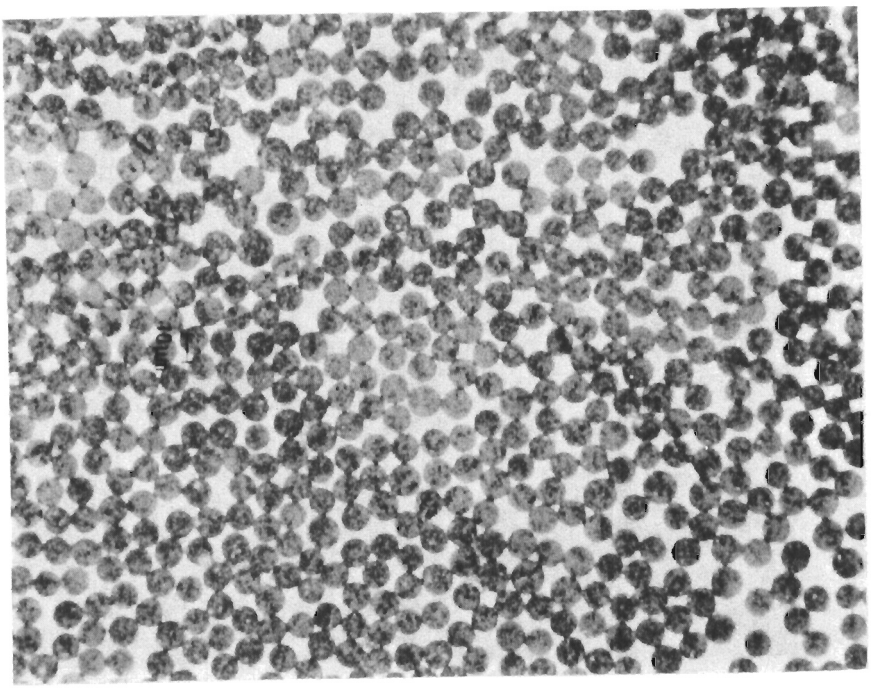

Figure 4. Cross Section of Control P-55 Gr/Mg Specimen

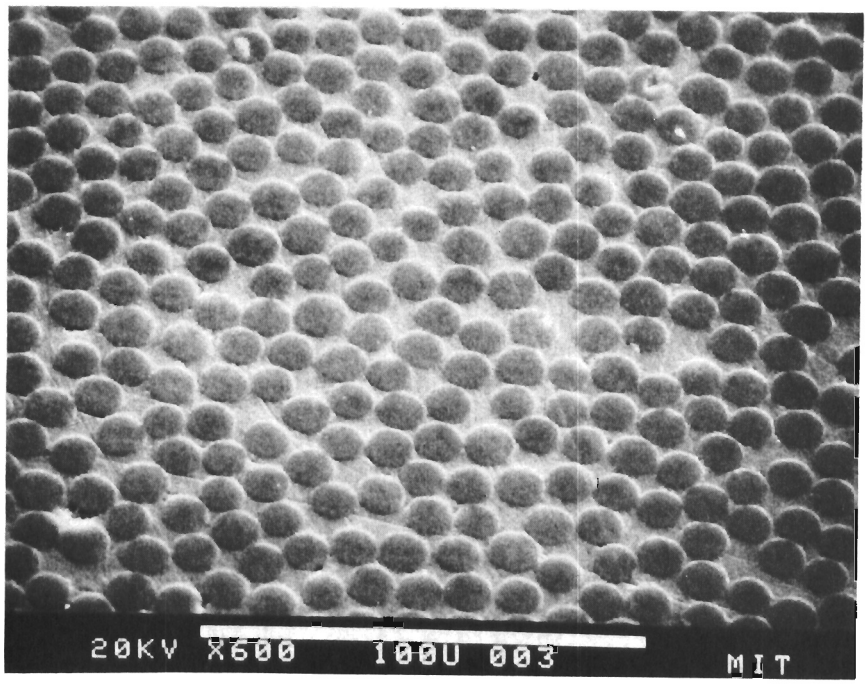

Figure 5. SEM of Control P-55 Gr/Mg Specimen

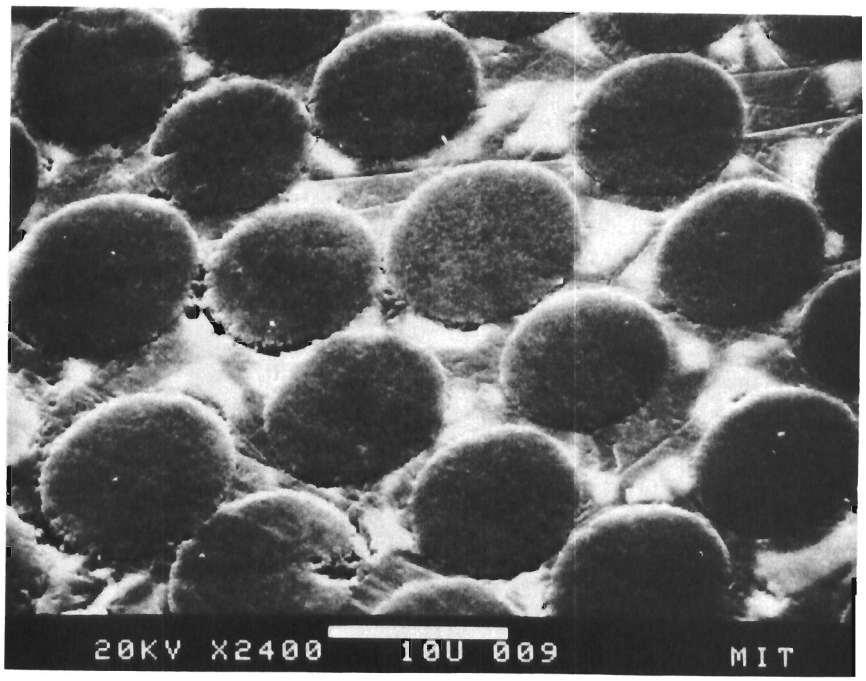

Figure 6. Zirconia-Dispersed Gr/Mg Specimen

Tensile Test Results:

Unidirectional P-55 Gr/Mg specimens exhibited tensile modulus at 35 Msi with strengths over 100 Ksi. This indicates a fiber content around 60 volume percent with no apparent fiber degradation. This represents a significant advance over current MMC technology. The zirconia-dispersed specimens exhibited tensile modulus at 30 Msi with average strength at 70 Ksi. These specimens showed reduced fiber-to-fiber contact points and are expected to possess improved transverse tensile strength, which is a critical need of current MMC technology.

Two each of control and zirconia-dispersed P-55 Gr/Mg specimens were strain-gauged and tensile-tested to failure following ASTM standards. A low strain rate (ε = 0.03/min) was maintained to simulate a static, tensile loading. The stress-strain curve was linear to failure in every case - the tensile modulus and strength values measured are presented in Table 2.

The modulus of the zirconia-dispersed specimens is about 15 percent lower than that of the control specimens. This is a result of lower reinforcement content (about 5 to 10 volume percent) and increased compliance due to interfacial slip phenomenon. The same factors also contribute to the reduced tensile strength for the zirconia-dispersed specimens.

Vibrational Testing and Results:

Damping measurement tests were conducted on cantilever specimens placed in an evacuated bell jar to eliminate aerodynamic damping. Flexural vibrations were initiated in the specimen by a solenoid-operated striker plate. A noncontacting fiber optic probe was used to measure displacements of specimen surface, and the displacement history of the specimen surface recorded at a high scan rate. A schematic diagram of the experimental setup is presented in Figure 7. The Fotonic 1000 system produced by MTRI Instruments, Inc., Latham, NY was used to noninvasively monitor the decaying amplitude of vibration. The system was configured to measure submicron (<0.04 mils) target surface displacements. Displacement data was collected at a high scan rate (7,431 Hz - about 30 times the specimen natural frequency) and stored in memory to calculate specimen damping.

Table 2. Results of the Tensile Tests

Specimen Number	Type	Modulus (Msi)	Ultimate Strain (%)	Ultimate Strength (Ksi)
1-1	Control	34.97	0.276	94.55
3-1	Control	35.07	0.348	119.83
2-1	With ZrO_2	28.93	0.185	59.5
4-1	With ZrO_2	30.86	0.25	79.3

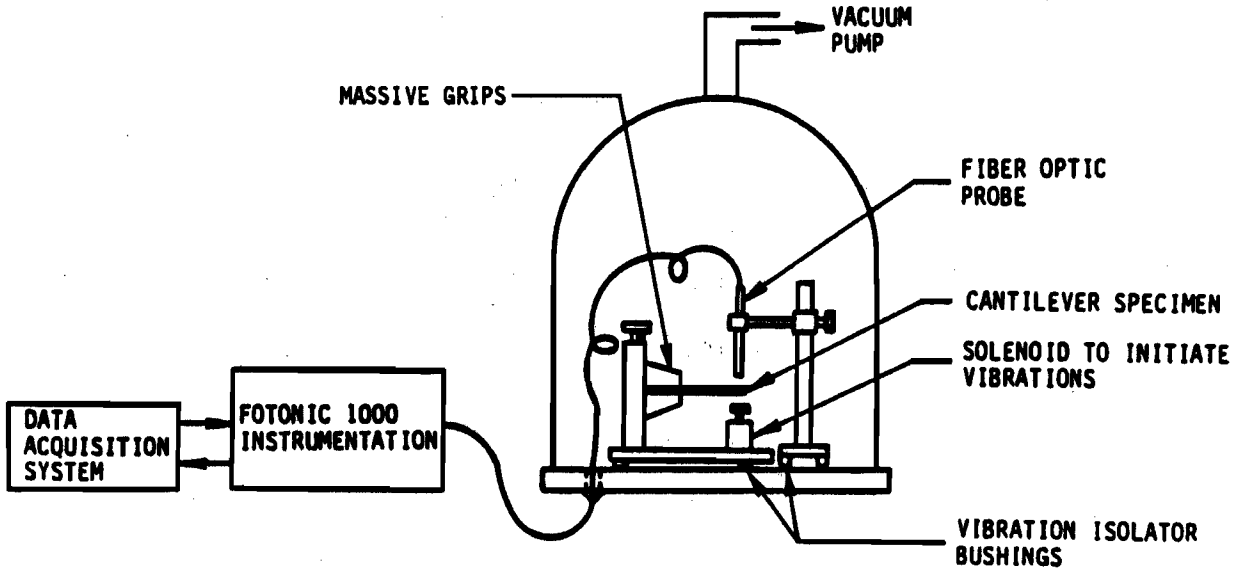

Figure 7. Schematic Representation of Test Setup

After initiation of vibrations, the specimens exhibited a decaying sinusoidal displacement response. The specific damping capacity ψ was calculated from amplitude decay over several hundred cycles using the relation

$$\psi = \frac{2}{j} \ln \frac{\alpha_1}{a_{1+j}}$$

where, the amplitude decays from α_1 to α_{1+j} over j consecutive cycles.

Six Gr/Mg specimens were tested to measure damping, with two specimens each of:

- Control - P-55/Mg, as-fabricated
- Annealed - P-55/Mg subsequently heat-treated
- Zirconia-dispersed - P-55/Mg with ~5 percent zirconia content.

In each case, electrical noise was controlled to a small fraction of the amplitude. Also, time-independence of the natural frequency was verified for each specimen. These displacement response curves were used to calculate specimen natural frequencies and strain levels using standard techniques - the results are presented in Table 3. Also, the specific damping capacity ψ was calculated using the procedure described earlier. Strain-dependence of damping for these specimens in the range 10^{-6} to 10^{-4} strain is illustrated in Figure 8.

Table 3. Summary of Vibration Characterization Test Results

Sample ID	Type	Natural Frequency, f_n (Hz)	Maximum Strain (ε_{max}) Initial	Final
1-1	Control	247.70	2.1×10^{-5}	4.5×10^{-6}
3-1	Control	206.42	2.6×10^{-5}	4.1×10^{-6}
3-3	Uncoated, annealed	206.42	1.9×10^{-5}	2.0×10^{-6}
3-2	Uncoated, annealed	206.42	1.6×10^{-5}	4.0×10^{-6}
4-1	With ZrO_2 dispersion	154.81	3.3×10^{-5}	2.7×10^{-6}
2-1	With ZrO_2 dispersion	195.55	2.5×10^{-5}	7.3×10^{-6}

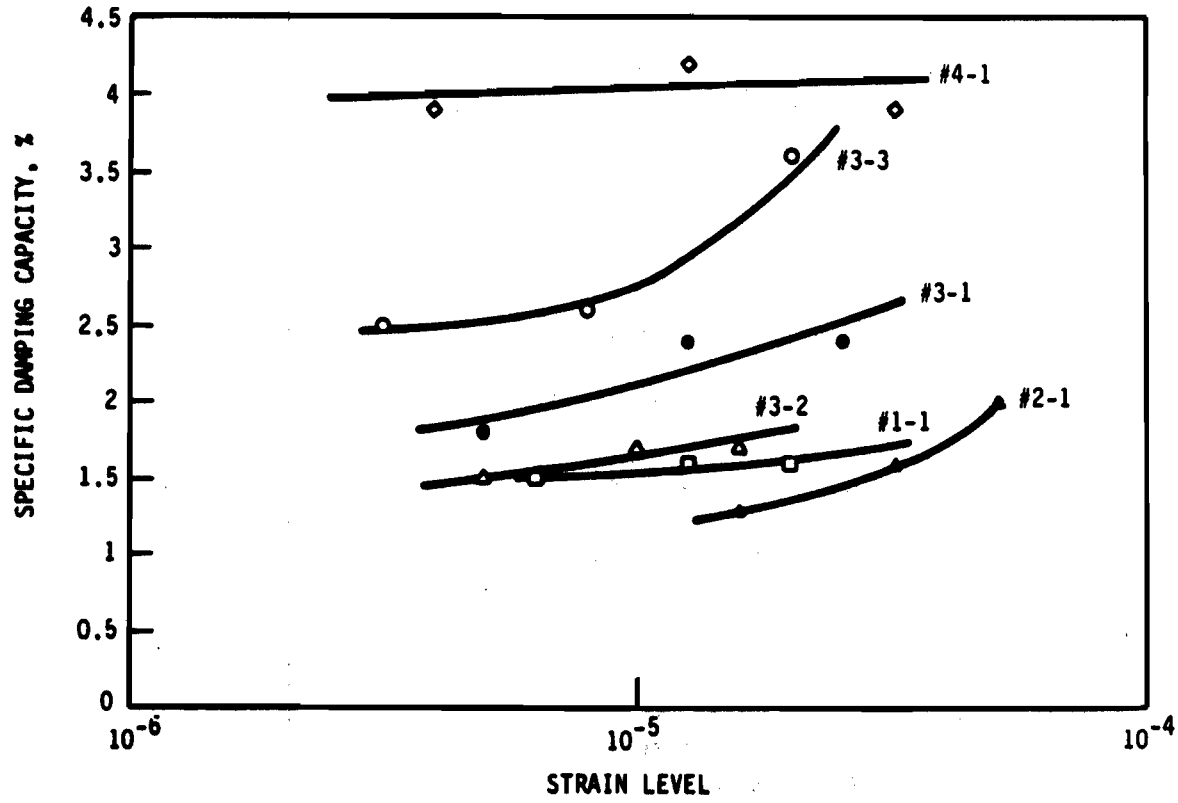

Figure 8. Strain-Dependence of Specific Damping Capacity for Various Specimens

The baseline damping value (strain-independent) for control specimens (No. 1-1, 3-1) is around 1.6 percent, which compares well with Martin Marietta data for Gr/Mg system.[9] The annealed specimens (No. 3-2, 3-3) show slight improvement in damping, with strain-independent damping close to 2.5 percent in specimen 3-3. The largest improvement in damping was exhibited by the zirconia-dispersed specimen (No. 4-1), with a strain-independent damping at 4 percent. The improvement in damping is expected to be the result of promoting interfacial slip through reduction in interface frictional coefficient and residual stresses. Unlike the dislocation damping mechanisms, the ISD mechanism improves damping at low strain levels ($<10^{-5}$), as seen in Figure 8. The other specimen in category (No. 2-1) did not exhibit interfacial slip mechanism, and consequently showed a strain-dependent damping similar to the control specimens. Thus, further work is necessary to promote ISD in MMCs with consistency. A parametric study must be conducted to understand the effect of fabrication process parameters, etc., on damping, followed by optimization of these parameters to maximize strain-independent damping. Also, the effect of vibration frequency and temperature on MMC damping must be characterized.

Settling Time Calculations:

Decay in amplitude of vibration for a freely vibrating component is obtained from the relation:

$$\alpha(t) = \alpha_0 e^{-\left(\frac{\psi\omega_n}{4\pi}\right)t}$$

where

$\alpha(t) \equiv$ amplitude as a function of time

$\alpha_0 \equiv$ amplitude at $t = 0$

$\psi \equiv$ specific damping capacity of material, assumed to be constant

$\omega_n \equiv$ natural frequency of component

$t \equiv$ time

Then, the settling time "t_s" is defined by the relation

$$t_s = \frac{4\pi}{\psi\omega_n} \ln \frac{\alpha_0}{\alpha_s}$$

where $\alpha_s \equiv$ acceptable amplitude of vibration in the component before firing.

These relations and the material properties measured were used to produce an amplitude decay representation for the flexural specimens after an impulse loading. In this calculation, only the strain-independent component of material damping was taken into consideration to represent low strain ($<10^{-5}$) behavior. Figure 9 presents the amplitude variation plots for Case 1 and Case 2. The decay in amplitude is much quicker for Case 2. To obtain a certain amplitude, α_s, was calculated using the same relation. Figure 10 presents the variation of (t_1/t_2) as a function of this acceptable amplitude, α_s. From this figure, a 75 to 90 percent reduction in settling time over current MMCs is projected, using the technology demonstrated during this research.

CONCLUSIONS

The strain-independent damping of Gr/Mg composites was improved by 150 percent by promoting the ISD mechanism. This was achieved through a zirconia dispersion with a low-effective modulus and specialized processing. The increased compliance resulted in a 5 to 50 percent reduction in the tensile modulus as compared to control specimens. Also, the reduced interface bond strength and stress concentrations caused by irregularly shaped zirconia regions were responsible for close to a 25 percent drop in the tensile strength as compared to control specimens. The drop in static mechanical properties can be reduced through a uniform compliant fiber coating.

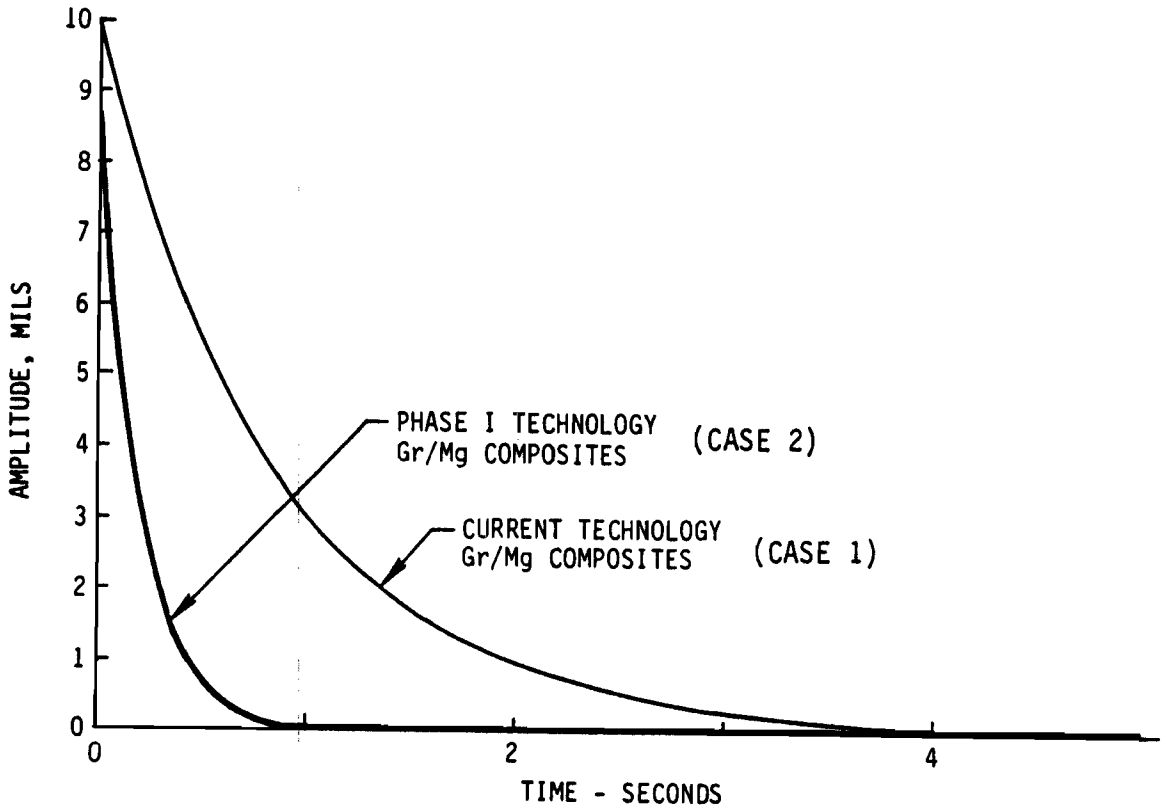

Figure 9. Amplitude Decay Representation in MMCs

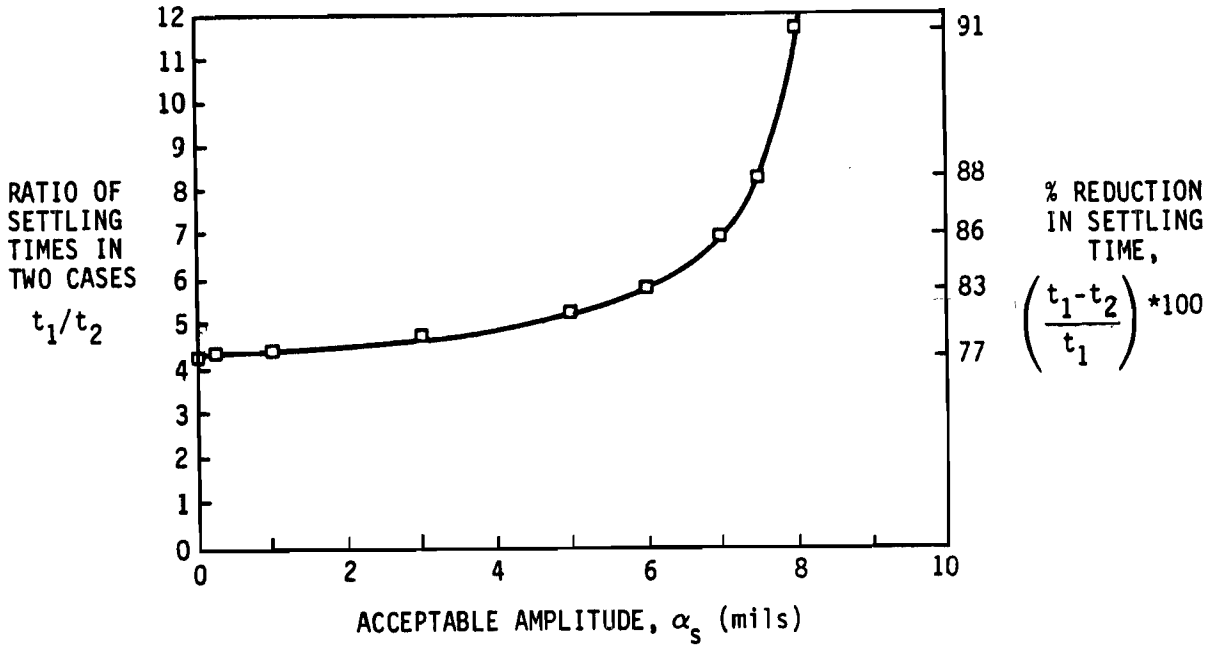

Figure 10. Reduction in Settling Time as a Function of Acceptable Amplitude

The major advantages of the ISD mechanism over the dislocation damping mechanism in MMCs are:

- ISD is effective in the low strain region ($<10^{-5}$) unlike dislocation damping.
- ISD is promoted by lowering residual stress in the MMC. This is expected to improve other dynamic properties, such as the fracture toughness and the fatigue strength. Dislocation damping is enhanced through high interface residual stresses which can deteriorate dynamic properties of the MMC.
- Dislocation damping is most effective in case of dislocation-prone matrix alloys which typically possess a low yield strength. This limitation will be reflected in the transverse properties of the MMC.

The interfacial slip mechanism needs to be researched further to obtain predictable improvements in vibrational damping. A parametric study will allow optimization of the process to minimize the deterioratory effect on static properties. Further, the effect of temperature, frequency and service time on the ISD mechanism must be characterized to develop suitable applications.

REFERENCES

1. Garibotti, J.F., C.J. Northrup, and A. Gunderson, "Design Aspects of MMC in SDI Spacecraft," Proceedings of Seventh MMC Technology Conference, Silver Springs, MD, May 1987.

2. Timmerman, N. and J. Doherty, Loss Factors Measured in Metal Matrix Composite Materials, NTIS Report No. ADA143542, June 1984.

3. Rawal, S.P. and M.S. Misra, "Material Damping in Space Structures," Damping 1986 Proceedings, AFWAL-TR-86-3059, May 1986.

4. Steckel, G., Material Damping Behavior of Gr/Mg Composites, Aerospace Corporation, El Segundo, CA, ONR Report No. TOR-0084-A-5726-01(-1), October 1985.

5. Nashif, A., D. Jones, and J. Henderson, Vibration Damping, Wiley-Interscience Publication, 1985.

6. Rawal, S.P., J.H. Armstrong, and M.S. Misra, Interfaces and Damping in Metal Matrix Composites, Martin Marietta Denver Aerospace Report No. MCR-86-684, December 1986.

7. Lazan, B.J., Damping of Materials and Members in Structural Mechanics, Permagon Press, Oxford, 1968.

8. Zener, C., Elasticity and Anelasticity of Metals, University of Chicago Press, Chicago, 1948.

9. Dr. Suraj Rawal, Martin Marietta, Denver, CO, Telephone Conversation, April 1988.

10. Kashalikar, U., "Highly Damped Gr/Mg Composites for Space Structures," Final Report, Contract No. N60921-87-C-0258, July 1988.